CDC25: A Component of the *RAS*–Adenylate Cyclase Pathway in *Saccharomyces cerevisiae*

LUCY C. ROBINSON, JACKSON B. GIBBS, MARK S. MARSHALL, IRVING S. SIGAL, KELLY TATCHELL

The yeast *Saccharomyces cerevisiae* contains two functional homologues of the *ras* oncogene family, *RAS1* and *RAS2*. These genes are required for growth, and all evidence indicates that this essential function is the activation of adenylate cyclase. In contrast, *ras* in mammalian cells does not appear to influence adenylate cyclase activity. To clarify the relation between *ras* function in yeast and in higher eukaryotes, and the role played by yeast *RAS* in growth control, it is necessary to identify functions acting upstream of *RAS* in the adenylate cyclase pathway. The evidence presented here indicates that *CDC25*, identified by conditional cell cycle arrest mutations, encodes such an upstream function.

MEMBERS OF THE MAMMALIAN *ras* oncogene family encode proteins, termed p21, that bind guanosine 5′-triphosphate (GTP) and guanosine 5′-diphosphate (GDP) and have low intrinsic GTPase activity. Oncogenic variants, altered at a limited number of amino acid positions, show significantly reduced GTPase activity without alteration of affinity for GTP and GDP, and a variant with increased nucleotide exchange is at least as potently transforming as viral *ras* (*1*). These properties, and the ability of p21 to associate with the plasma membrane, resemble properties of guanine nucleotide-binding regulatory proteins (G proteins) that are associated with a number of signal transduction systems (*2*). The idea that *ras* may act as a G protein is supported by evidence linking *ras* with the action of growth hormones (*3*, *4*), although the signal transduction system activated by *ras* does not appear to be adenylate cyclase (*5*).

Two *ras* homologues in the yeast *Saccharomyces cerevisiae*, *RAS1* and *RAS2*, encode related proteins with the same biochemical properties as their vertebrate counterparts (*6*). Yeast *RAS* is also functionally homologous with mammalian *ras*. This homology is illustrated by the ability of mammalian and viral *ras* genes to substitute for the essential function of yeast *RAS* (*7*, *8*), and by the ability of a reconstructed yeast *RAS* gene to transform mammalian cells, but only after the unique 118-residue COOH-terminal domain has been removed and the position analogous to the oncogenic leu61 mutation has been altered (*7*). Genetic and biochemical evidence indicates that yeast *RAS* stimulates adenylate cyclase activity (*9*, *10*). The functional homology of yeast and mammalian *ras* suggests that although interacting proteins in the two systems may not be identical, such proteins may have conserved domains. The identification of these proteins is important not only for understanding *RAS* function in yeast, but also potentially for clues to the nature of the signals mediated by mammalian *ras*.

In yeast, stimulation of adenylate cyclase activity plays a pivotal role in control of vegetative growth (*11*). Cells with constitutively increased adenylate cyclase activity caused by either adenylate cyclase mutations or the dominant $RAS2^{val19}$ mutation (analogous to position-12 transforming mutations in mammalian *ras*) fail to respond to deprivation of nutrients. Diploids carrying these mutations fail to accumulate glycogen and do not sporulate at wild-type levels; both defects are in response to starvation. Cells lacking adenylate cyclase or *RAS* activity are inviable; the terminal phenotype of such cells is arrest during the prereplicative phase (G1) of the cell cycle. The loss of *RAS2* alone is not lethal, but it results in several defects, including an inability to grow on nonfermentable carbon sources and, in the homozygous diploid, a lack of nutrient repression of sporulation, termed hypersporulation (*12*). Mutations suppressing the former defect have been isolated in our laboratory, and among the characteristics of several of these is the ability to suppress the temperature-sensitive (ts) G1 arrest of two cell division cycle (cdc) mutations, *cdc25* and *cdc35* (*13*). The suppression of *cdc35* was expected since *cdc35* is known to be a ts allele of the adenylate cyclase structural gene (*14*). The suppression of *cdc25* by the same set of mutations suggested that *CDC25* encodes a component of the same pathway. This is supported by two facts: that *cdc25* ts arrest can be suppressed by exogenous adenosine 3′,5′-monophosphate (cAMP) and that *cdc25* mutants show altered intracellular cAMP levels at the restrictive temperature (*15*).

To further examine the relation between *CDC25* and *RAS*, we have tested the effect of the activating mutation $RAS2^{ala18val19}$ (*16*) on the phenotypes of *cdc25* and *cdc35* mutants. We found that *cdc35* was epistatic to $RAS2^{ala18val19}$, which is consistent with *RAS* activation of adenylate cyclase. In contrast, $RAS2^{ala18val19}$ eliminates the growth requirement for *CDC25*. Additionally, the activity of adenylate cyclase was greatly reduced in *cdc25-1* mutants but was restored to wild-type levels when $RAS2^{ala18val19}$ was also present. These results confirm that *CDC25* acts in the *RAS*–adenylate cyclase pathway and allow us to place this function upstream of *RAS*.

$RAS2^{ala18val19}$ was initially tested for suppression of the ts-arrest phenotype of *cdc25-1* and of *cdc35-10*. *RAS2* and $RAS2^{ala18val19}$ were cloned in the yeast centromere-containing vector YCp50, with the selectable marker *URA3*, for these experiments because this vector is maintained at low copy

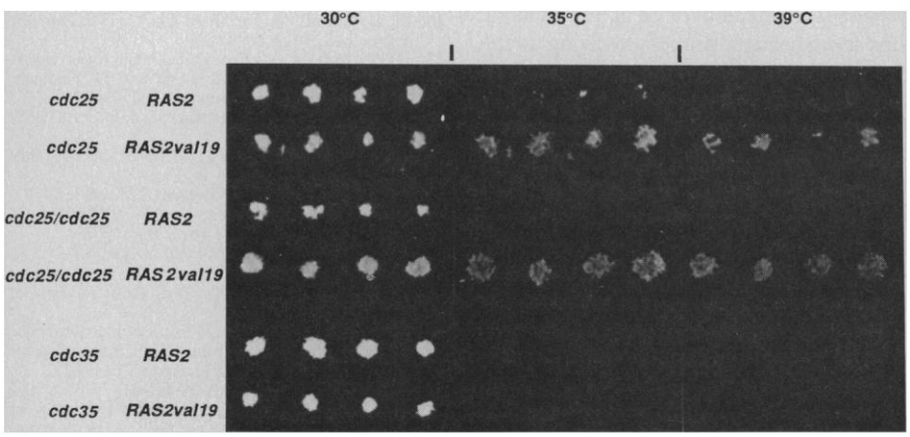

Fig. 1. Effect of $RAS2^{ala18val19}$ on the ability of *cdc25* and *cdc35* strains to grow at restrictive temperatures. Master plates incubated at 25°C were replica-plated to plates incubated at 30°, 35°, and 39°C. The *cdc35-10* strain used was LR501; the *cdc25-1* strains used were LR400 and LR433. Plasmids used were p*RAS2* and $pRAS2^{ala18val19}$. Selective media were prepared and yeast was cultured as described (*22*, *23*), and yeast transformation was carried out as described by Beggs (*25*).

L. C. Robinson and K. Tatchell, Department of Biology, University of Pennsylvania, Philadelphia, PA 19104. J. B. Gibbs, M. S. Marshall, I. S. Sigal, Department of Virus and Cell Biology, Merck Sharp & Dohme Research Laboratories, West Point, PA 19486.

Table 1. Effect of *RAS2*^{ala18val19} on sporulation. Diploids homozygous for *cdc35-10* were constructed by crossing the LR501 transformants described in the text to LR510 (*a ade2 leu2 ura3-1 cdc35-10*). Diploids homozygous for *cdc25-1* were generated by transformation of LR600 (*a/α ade2/ade2 his4/his4 leu2/leu2 ura3-52/ura3-52 cdc25-1/cdc25-1*) with *pRAS2* and *pRAS*^{ala18val19}. Diploids were sporulated on conventional KAc sporulation medium and, to score hypersporulation, on media containing 2% yeast extract, 2% peptone, and 3% glycerol as carbon source (YEPG). The overall sporulation efficiency of the *cdc25* diploids is lower than that of *cdc35* diploids as a result of preincubation of *cdc25* strains on minimal medium lacking uracil for 48 hours before transfer to sporulation media, whereas *cdc35* strains were incubated on rich medium containing 2% yeast extract, 2% peptone, and 2% glucose (YEPD). This preincubation was used for *cdc25* strains to ensure that the asci counted for *pRAS2*^{ala18val19} diploids resulted from meiosis of cells retaining the plasmid, since progeny obtained under these conditions, but not with preincubation on YEPD, included plasmid-bearing cells. Media used for scoring selective markers and for sporulation have been described (*22, 23*). All sporulation counts were carried out after 72 hours at 30°C on the indicated medium. Only three- and four-spored asci were counted, and the percentage given is the average of three trials; at least 500 cells were counted per trial.

Strain	Relevant genotype	Sporulation (%)	
		YEPG	Spor
LR650	*cdc35-10/cdc35-10*	42	65
LR650/p*RAS2*	*cdc35-10/cdc35-10*	36	64
LR650/ p*RAS2*^{ala18val19}	*cdc35-10/cdc35-10*	37	56
LR600	*cdc25-1/cdc25-1*	7	42
LR600/p*RAS2*	*cdc25-1/cdc25-1*	6	38
LR600/ p*RAS2*^{ala18val19}	*cdc25-1/cdc25-1*	0.8	4.5

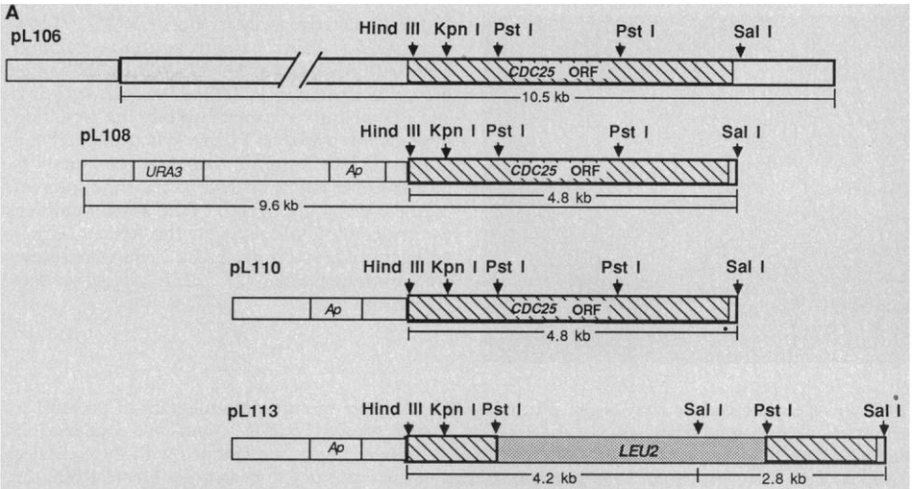

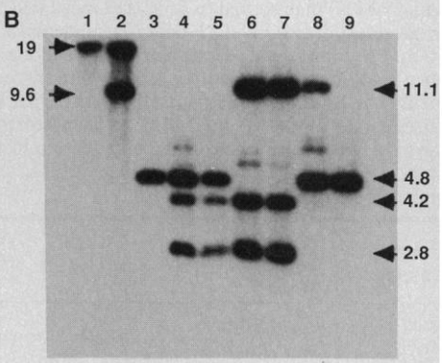

Fig. 2. Cloning and disruption of *CDC25*. (**A**) Restriction maps of plasmids used. pL106 was isolated from a YCp50 yeast genomic library by complementation of the *cdc25-1* ts arrest phenotype. The 4.8-kb Sal I–Hind III restriction fragment from pL106 was subcloned in the integrating vector Ylp5 to yield pL108. To confirm that this fragment contained *CDC25* sequences, pL108 was linearized with Kpn I and used to transform LR469-9C (*a leu2 met3 ura3-52*) to Ura$^+$. The pL108 integrant LR603c was crossed to LR400 and the diploid sporulated for tetrad analysis. Among the 31 tetrads examined, no spore clone recombinant for *cdc25-1* and the Ura$^+$ phenotype was recovered, which indicates that the Sal I–Hind III fragment directed integration of pL108 by homology less than 1.6 cM from the *CDC25* locus. For disruption of *CDC25*, the Sal I–Hind III fragment was cloned in pUC9 (pL110) and the 1.7-kb Pst I fragment was replaced with the 4-kb *LEU2* Pst I fragment (pL113). (**B**) Southern blot analysis of DNA from wild-type strains and from integrative transformants with pL108 and pL113. Lanes 1 and 2 are Sal I digests of DNA from the wild-type strain LR469-9C and the pL108 integrant LR603c, respectively. The lower molecular weight band of hybridization in lane 2 represents the integrated vector sequences, as shown above. Lanes 3 through 9 are Sal I + Hind III digests of DNA prepared from: lane 3, LR600; lanes 4 and 5, *cdc25-113:LEU2* heterozygotes LR601a and LR601b; lanes 6 and 7, *cdc25-113:LEU2* haploid segregants LR602d-5B and LR602a-3D; lanes 8 and 9, *cdc25-1* haploid segregants LR602a-3A and LR602a-3C. The major bands of hybridization marked correspond to the sizes indicated in (A). Lanes 4 through 6 also show strong hybridization at 11.1 kb. This is the size expected for the Sal I–Hind III digest of p*RAS2*^{ala18val19}; both the 11.1-kb fragment and the probe contained pBR322 DNA. Genomic DNA prepared as described (*26*) was digested with a threefold excess of the indicated restriction enzyme(s), fractionated on a 0.7% agarose gel (*26*), and transferred to a nitrocellulose filter (*27*). The filter was hybridized under conditions described by Tatchell *et al.* (*28*) to pL110 that was labeled with ^{32}P by nick translation (*29*). Sizes are shown in kilobases.

number (*17*). Haploid *cdc25* and *cdc35* strains LR400 (*a ade2 his4 leu2 tyr1 ura3-52 cdc25-1*) and LR501 (*a leu2 ura3-52 cdc35-10*) were transformed with p*RAS2*^{ala18val19} or p*RAS2*. Ura$^+$ transformants were tested for growth at 35°C, the restrictive temperature for both *cdc25* and *cdc35*. The *cdc35* strain transformed with either p*RAS2* or p*RAS2*^{ala18val19} remained ts (Fig. 1). The *cdc25* strain transformed with p*RAS2* also remained ts, but the same strain transformed with p*RAS2*^{ala18val19} no longer showed the *cdc* phenotype; instead, these transformants grew at temperatures as high as 39°C. Reversion of *cdc25-1* in the latter strain was ruled out by the fact that loss of the plasmid (as judged by the Ura$^-$ phenotype) was accompanied by loss of ability to grow at 35°C.

RAS2^{ala18val19} confers a dominant sporulation-deficient (spo−) defect (*9*). In contrast, *cdc25* and *cdc35* cause the recessive hypersporulation phenotype also seen for *ras2* mutants; that is, diploids homozygous for either mutation sporulate on rich media (*18*). Strains of the genotype *cdc35/cdc35* p*RAS2*^{ala18val19} show the hypersporulation characteristic of *cdc35*. In contrast, sporulation of a *cdc25/cdc25* p*RAS2*^{ala18val19} strain was only one-tenth that of a congenic *cdc25/cdc25* strain (Table 1).

As would be expected if *RAS* activates adenylate cyclase, *cdc35* is epistatic to *RAS2*^{ala18val19}. The suppression of the *cdc25-1* ts arrest phenotype at temperatures as high as 39°C by *RAS2*^{ala18val19} suggests that *CDC25* is a component of the *RAS*–adenylate cyclase pathway and that *RAS2*^{ala18val19} bypasses the requirement for *CDC25* activity. To determine directly whether loss of *CDC25* function affects the adenylate cyclase pathway, we compared the adenylate cyclase activities in membrane preparations from *cdc25-1* and *CDC25* strains transformed with p*RAS2* or p*RAS2*^{ala18val19}. The *RAS*-dependent adenylate cyclase activity, assayed with Mg^{2+}, in the *cdc25-1* strain transformed with either YCp50 or p*RAS2* was markedly reduced from the wild type (Table 2). In contrast, the same strain transformed with p*RAS2*^{ala18val19} showed wild-type adenylate cyclase activity. In the presence of Mn^{2+}, all strains had a readily measurable activity that varied by a factor of 2 to 3. The impaired basal *RAS*-dependent adenylate cyclase activity in the *cdc25-1* strain transformed with YCp50 or p*RAS2* was further evident when the activity assayed with Mg^{2+} was compared with the catalytic activity assayed in the presence of Mn^{2+} (Table 2). These results further support the hypothesis that

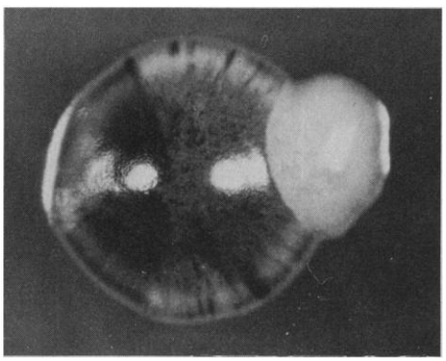

Fig. 3. Qualitative analysis of p*RAS2*^{ala18val19} loss from *cdc25-113:LEU2* strains by iodine staining. LR602d-5B, a haploid *cdc25-113:LEU2* segregant, was crossed to JC482 (*a his4 leu2 ura3-52*), and the mixture of parent haploids and resulting diploids was plated on YEPD. When colonies had grown to 1 to 2 mm in diameter, the plate was inverted over iodine crystals to stain the colonies on the basis of glycogen content. Dark sectors in the larger diploid colony to the left are Ura$^-$, whereas no dark sectors or Ura$^-$ cells were recovered from the *cdc25-113:LEU2* haploid colony (right).

Table 2. Adenylate cyclase activity (in picomoles of cAMP per minute per milligram of protein) in membrane preparations from *cdc25-1* and *CDC25* strains. Strains LR599 (*a ade2 his4 leu2 ura3-52 cdc25-1*) and KT112 (α *ade2-1 can1-100 his3 leu2-3.112 ura3-1*) were transformed with the indicated plasmids. Cells were grown at 26°C in minimal medium without uracil to an absorbance at 600 nm (A_{600}) of 0.5, then shifted to 35°C and incubated for 2 hours. A membrane fraction was then prepared by glusulase digestion and Dounce homogenization of the resulting spheroplasts in buffer containing 50 m*M* sodium (2-[*N*-morpholino]ethanesulfonate), *p*H 6.0, 0.1 m*M* EGTA, 0.1 m*M* $MgCl_2$, 1 m*M* phenylmethyl-sulfonyl fluoride, 1 m*M* dithiothreitol, followed by centrifugation at 105,000*g* for 30 minutes at 4°C. Adenylate cyclase assays were performed at 25°C for 40 minutes as described (*24*) with 10 m*M* $MgCl_2$ or 0.7 m*M* $MnCl_2$. Data are the means ± SD of four determinations from three experiments or the average of duplicate determinations from a single experiment. The reduced activity observed for KT112 transformed with p*RAS2*^{ala18val19} parallels the growth-retarding effect of this mutation in this strain.

Relevant genotype	Plasmid	Activity (pmol min^{-1} mg^{-1})		Ratio
		Mg^{2+}	Mn^{2+}	Mn^{2+}/Mg^{2+}
cdc25-1	YCp50	0.8 ± 1.0	38.6	48
cdc25-1	p*RAS2*	1.0 ± 0.6	39.1	39
cdc25-1	p*RAS2*^{ala18val19}	11.7 ± 2.2	130	11
CDC25	YCp50	14.4 ± 3.2	80.5	5.6
CDC25	p*RAS2*	17.7 ± 6.1	83.3	4.7
CDC25	p*RAS2*^{ala18val19}	4.5 ± 1.3	39.6	8.8

CDC25 is a component of the *RAS*–adenylate cyclase pathway.

To test the hypothesis that *RAS2*^{ala18val19} eliminates the requirement for *CDC25* activity, we determined the effect of this mutation on the phenotype of a *CDC25* disruption mutation. The *CDC25* gene was cloned as described in Fig. 2A. A YCp50 plasmid from a yeast genomic library, pL106 (Fig. 2A), complements the *cdc25-1* ts phenotype. A 4.8-kb Sal I–Hind III restriction fragment from pL106 directs integration by homology less than 1.6 centimorgans (cM) from the *CDC25* locus and has a restriction map similar to that reported for *cdc25* (*15*, *19*). A null allele of *CDC25*, *cdc25-113:LEU2* (Fig. 2A) was generated in vitro by inserting a restriction fragment containing the *LEU2* gene into an internal *CDC25* deletion and was introduced into the chromosome by gene replacement as described by Rothstein (*20*). The plasmid pL113 (Fig. 2A) was digested with Pvu II and Hind III, and the 7-kb fragment containing the disrupted *CDC25* gene was purified and used to transform the diploid strain LR600 (*cdc25/cdc25 leu2/leu2*) to Leu$^+$. Southern analysis of stable Leu$^+$ transformants showed two diploids, LR601a and LR601b, to be heterozygous for the *cdc25-113:LEU2* disruption (Fig. 2B, lanes 4 and 5). When these strains were sporulated, each gave rise to only two viable meiotic products per ascus, both of which were Leu$^-$ and therefore carried *cdc25-1* rather than *cdc25-113:LEU2*. The two nongrowing spores of each tetrad did not bud.

The inability to recover Leu$^+$ (*cdc25-113:LEU2*) haploid segregants indicates that *CDC25* function is essential for growth. To test whether the requirement for *CDC25* could be eliminated by *RAS2*^{ala18val19}, LR601b, a diploid heterozygous for the *cdc25-113:LEU2* disruption, was transformed to Ura$^+$ with p*RAS2*^{ala18val19} or p*RAS2* and sporulated for tetrad analysis. Haploid Leu$^+$ Ura$^+$ (*cdc25-113:LEU2* p*RAS*) segregants were recovered in the progeny of *RAS2*^{ala18val19} but not *RAS2* transformants. Southern analysis of these strains confirmed the presence of the *cdc25-113:LEU2* disruption (Fig. 2B, lanes 6 and 7).

The presence of haploid *cdc25-113:LEU2* segregants in the progeny of *RAS2*^{ala18val19} but not *RAS2* transformants suggests that the *RAS2*^{ala18val19} mutation is responsible for, and required for, the growth of these strains. Consistent with this idea, we recovered no Leu$^+$ Ura$^-$ colonies after growth of haploid Leu$^+$ Ura$^+$ strains on media containing uracil. To ensure that this observation reflects a requirement for the plasmid for viability rather than abnormally high stability of p*RAS2*^{ala18val19}, we examined the behavior of this plasmid in diploid strains heterozygous for *cdc25-113:LEU2*. The plasmid should not be required for viability of the heterozygous diploid and therefore should be lost at the low-frequency characteristic of centromere plasmids. *RAS2*^{ala18val19} strains do not accumulate glycogen and thus stain light or yellow with iodine, whereas wild-type and *cdc25* strains stain brown. This differential staining allowed us to score plasmid stability qualitatively within a single colony. The haploid colony to the right in Fig. 3 is uniformly light, indicating retention of p*RAS2*^{ala18val19}. This strain was crossed with a *CDC25*$^+$ strain, and the resulting diploid, to the left in Fig. 3, shows numerous dark sectors that reflect the loss of p*RAS2*^{ala18val19}.

This preliminary analysis of the *cdc25-113:LEU2* disruption indicates that the *CDC25* product is essential for growth. Spores receiving the disrupted allele do not bud, and haploid *cdc25-113:LEU2* strains carrying the plasmid-borne suppressor mutation *RAS2*^{ala18val19} become inviable when the plasmid is lost. The suppression of *cdc25-113:LEU2* lethality by p*RAS2*^{ala18val19} confirms that the activated *RAS2* eliminates the requirement for *CDC25* function. Thus, although *cdc35* is epistatic to *RAS2*^{ala18val19} by all criteria examined, the reverse is true for *cdc25*.

The proposed role for *RAS* in yeast resembles that of a stimulatory G protein for adenylate cyclase. According to this model, the GTP-bound form of *RAS* is active, and hydrolysis to the GDP-bound form reduces activity. Consistent with this model, *RAS-2*^{val19} mutants resemble constitutive adenylate cyclase mutants (*8*, *9*), and *RAS2*^{val19} protein activates adenylate cyclase constitutively in vitro (*10*). Our results with *cdc35* are also consistent with this model since *RAS2*^{val19} should have no effect in strains with an inactive adenylate cyclase. In contrast, the bypass of *CDC25* function by *RAS2*^{ala18val19} and the restoration of adenylate cyclase activity in *cdc25-1* strains to wild-type levels indicate that *CDC25* acts upstream of *RAS* in this pathway.

There is no clear evidence as to the nature of the signals mediated by the *RAS*–adenylate cyclase pathway in yeast. The phenotypes of *RAS* and adenylate cyclase mutants suggest that this pathway responds to nutritional conditions. Signal transduction

through *RAS* would be effected by a factor responsive to nutritional signals, which could facilitate exchange of guanine nucleotides on *RAS*. Although there is no evidence that such a factor acts on *RAS*, proteins providing guanine nucleotide exchange activity are known for hormone-responsive G proteins (*2*) and for translation factors EF-Tu and elF-2 (*21*). Like these proteins, *RAS* binds GDP and GTP with high affinity (*1*).

The only apparent biochemical difference between *RAS2* and *RAS2*^{val19} proteins is the reduction of GTPase activity of the latter. The active form of *RAS2*^{val19} would therefore have an extended half-life and could require less exchange factor activity to remain stimulatory. Alternatively, published data suggests that the GDP-bound form of *RAS2*^{val19} may be as active as the GTP adduct of *RAS2* (*10*), which would also reduce the need for GTP-GDP exchange. The ability of the activated form of *RAS2* to suppress the lethality of the *cdc25* disruption allele therefore raises the possibility that *CDC25* could act as a guanine nucleotide exchange factor for *RAS*. However, the sequence of *CDC25* has been determined, and a comparison of the predicted amino acid sequence with known proteins and translated open reading frames was reported to give no significant homologies (*15*). Direct evidence that the *CDC25* gene product functions as a modulator of *RAS* activity, whether as a GTP exchange factor or through an as yet unknown activity, awaits genetic and biochemical analysis of *CDC25* mutations.

REFERENCES AND NOTES

1. J. B. Gibbs, I. S. Sigal, E. M. Scolnick, *Trends Biochem. Sci.* **10**, 350 (1985); I. S. Sigal *et al.*, *Proc. Natl. Acad. Sci. U.S.A.* **83**, 952 (1986).
2. A. G. Gilman, *Cell* **36**, 577 (1984).
3. N. Hagag, S. Halegoua, M. Viola, *Nature (London)* **319**, 680 (1986).
4. D. Bar-Sagi and J. Feramisco, *Cell* **42**, 841 (1985).
5. S. K. Beckner, S. Hattori, T. Shih, *Nature (London)* **317**, 71 (1985).
6. F. Tamanoi, N. Samiy, M. Rao, M. Walsh, in *Cancer Cells III: Growth Factors and Transformation*, J. Feramisco, B. Ozanne, L. Stiles, Eds. (Cold Spring Harbor Laboratory, Cold Spring Harbor, NY, 1985), pp. 251–256; G. L. Temeles *et al.*, *Nature (London)* **313**, 700 (1985).
7. D. DeFeo-Jones *et al.*, *Science* **228**, 179 (1985).
8. T. Kataoka *et al.*, *Cell* **40**, 19 (1985).
9. T. Toda *et al.*, *ibid.*, p. 27.
10. D. Broek *et al.*, *ibid.* **41**, 763 (1985).
11. K. Matsumoto, I. Uno, T. Ishikawa, *Yeast* **1**, 15 (1985).
12. K. Tatchell, L. C. Robinson, M. Breitenbach, *Proc. Natl. Acad. Sci. U.S.A.* **82**, 3785 (1985); D. Fraenkel, *ibid.*, p. 4740.
13. J. Cannon, J. B. Gibbs, K. Tatchell, *Genetics* **113**, 247 (1986); L. C. Robinson, unpublished results.
14. F. Boutelet, A. Petitjean, F. Hilger, *EMBO J.* **4**, 2635 (1985).
15. J. H. Camonis *et al.*, *ibid.* **5**, 375 (1986).
16. The activating *RAS2*^{ala18val19} mutation was created by in vitro mutagenesis [J. B. Gibbs, I. S. Sigal, M. Poe, E. M. Scolnick, *Proc. Natl. Acad. Sci. U.S.A.* **81**, 5704 (1984)]. The replacement of the glycine residue at position 18 by alanine reflects the normal cellular *ras* sequence, and the replacement of glycine at position 19 by valine is the activating mutation, analogous to valine at position 12 in mammalian *ras*. *RAS2*^{ala18val19} is similar to *RAS2*^{val19} by all criteria examined.
17. M. Johnston and R. Davis, *Mol. Cell. Biol.* **4**, 1440 (1984).
18. V. Shilo, G. Simchen, B. Shilo, *Exp. Cell Res.* **112**, 241 (1978).
19. E. Martegani, M. Baroni, G. Frascotti, L. Alberghina, *EMBO J.* **5**, 2363 (1986).
20. R. J. Rothstein, *Methods Enzymol.* **101**, 202 (1983).
21. S. M. Hughes, *FEBS Lett.* **164**, 1 (1983).
22. R. K. Mortimer and D. C. Hawthorne, in *The Yeasts*, A. H. Rose and J. S. Harrison, Eds. (Academic Press, New York, 1969), vol. 1, pp. 385–460.
23. K. Tatchell *et al.*, *Cell* 27, 25 (1981).
24. G. Casperson *et al.*, *J. Biol. Chem.* **258**, 7911 (1983).
25. J. D. Beggs, *Nature (London)* **275**, 104 (1978).
26. F. Winston, F. Chumley, G. R. Fink, *Methods Enzymol.* **101**, 211 (1983).
27. T. Maniatis, A. Jeffrey, H. Van de Sande, *Biochemistry* **14**, 3787 (1975).
28. K. Tatchell, D. T. Chaleff, D. DeFeo-Jones, E. M. Scolnick, *Nature (London)* **309**, 523 (1984).
29. G. M. Wahl, M. Stern, G. Stark, *Proc. Natl. Acad. Sci. U.S.A.* **76**, 3683 (1979).

30. We thank F. Hilger for providing a *cdc35-10* strain, M. Rose for providing the YCp50 yeast genomic library, and S. Poethig and J. Cannon for critical reading of the manuscript. Supported in part by grant CA37702 from the National Cancer Institute. L.C.R. was supported by NIH predoctoral training grant GM07229.

17 September 1986; accepted 30 December 1986

Xenopus Oocytes Injected with Rat Uterine RNA Express Very Slowly Activating Potassium Currents

M. B. BOYLE, E. M. AZHDERIAN, N. J. MACLUSKY, F. NAFTOLIN, L. K. KACZMAREK

Under the influence of estrogen, uterine smooth muscle becomes highly excitable, generating spontaneous and prolonged bursts of action potentials. In a study of the mechanisms by which this transition in excitability occurs, polyadenylated RNA from the uteri of estrogen-treated rats was injected into *Xenopus* oocytes. The injected oocytes expressed a novel voltage-dependent potassium current. This current was not observed in oocytes injected with RNA from several other excitable tissues, including rat brain and uterine smooth muscle from ovariectomized rats not treated with estrogen. The activation of this current on depolarization was exceptionally slow, particularly for depolarizations from relatively negative membrane potentials. Such a slowly activating channel may play an important role in the slow, repetitive bursts of action potentials in the myometrium.

THE SMOOTH MUSCLE OF THE UTERUS, the myometrium, in common with many neuronal systems (*1*), undergoes long-lasting changes in electrical excitability. Estrogen treatment of the adult uterus causes growth of the myometrium and the appearance of spontaneous electrical activity consisting of prolonged bursts of action potential firing lasting many seconds (*2*). Little is known about the ionic mechanisms that underlie such slow electrical events, in part because of the technical difficulties associated with studying smooth muscle cells. We have used the *Xenopus* oocyte translation system (*3–6*) to detect mRNA (messenger RNA) coding for ion channels in uterine smooth muscle. Previous work by Dahl and co-workers (*6*) has shown that RNA from uterus can be used to express gap-junction proteins. We here describe a novel voltage-dependent potassium current observed in frog oocytes injected with polyadenylated [poly(A)$^+$] RNA from the uterine horns of rats treated with estrogen.

Actively cycling, adult female Sprague-Dawley rats (Charles River) were ovariectomized and implanted with Silastic capsules containing 100% β-estradiol (*7*). After 3 days, the animals were killed, and RNA was prepared from the uterine horns (*8*). *Xenopus* oocytes were injected with 200 ng of poly(A)$^+$ RNA in 50 nl of sterile water. Control oocytes were injected with 50 nl of sterile water. After incubation for 3 days the oocytes were voltage-clamped at 20° to 23°C by the use of conventional two-microelectrode techniques (*9*).

Figure 1 shows voltage-clamp records obtained from an oocyte 3 days after injection of 200 ng of uterine poly(A)$^+$ RNA. Depolarizations from a holding potential of −40 mV elicited a voltage- and time-dependent outward current, first evident at −30 mV. On repolarization to −40 mV, large, slowly decaying outward tail currents were observed. Similar outward currents were re-

M. B. Boyle and E. M. Azhderian, Department of Pharmacology, Yale University School of Medicine, New Haven, CT 06510.
N. J. MacLusky, Departments of Pharmacology and Obstetrics and Gynecology, Yale University School of Medicine, New Haven, CT 06510.
F. Naftolin, Department of Obstetrics and Gynecology, Yale University School of Medicine, New Haven, CT 06510.
L. K. Kaczmarek, Departments of Pharmacology and Physiology, Yale University School of Medicine, New Haven, CT 06510.